International Journal of Engineering Trends and Technology
ISSN: 2231 – 5381 / https://doi.org/10.14445/22315381/IJETT-V70I8P220

Volume 70 Issue 8, 194-205, August 2022

Original Article

A Novel Method for Implementing MPPT Based Photovoltaic Closed Loop Flyback Inverter with STM32F407VG Controller using Waijung Tool

Mangala R. Dhotre[1], Prashant V. Thakre[2], Vijay M. Deshmukh[3]

[1]*Electronics and Telecommunication Department, Government College of Engineering, Jalgaon, Maharashtra, India.*
[2]*Electrical Department, Tulsiramji Gaikwad Patil College of Engineering and Technology, Nagpur, Maharashtra, India.*
[3]*Electronics and Telecommunication Department, SSBT's College of Engineering and Technology, Bambhori, Jalgaon, Maharashtra, India.*

[1]*mangala_dev@rediffmail.com*

Received: 15 June 2022 Revised: 31 July 2022 Accepted: 11 August 2022 Published: 22 August 2022

Abstract *- Nowadays, renewable energy sources are continuously increasing to reduce global warming. Since solar energy is abundantly available in India, the proposed model uses a photovoltaic (PV) system to generate dc input voltage applied to a system. Flyback inverters are gaining more popularity due to their simplicity, low cost, and high efficiency. To increase the use of flyback inverters, this research presents a novel method for implementing a photovoltaic-based closed-loop flyback inverter using an STM32F407VG digital controller in the wiajung platform. The system consists of a photovoltaic system, a flyback inverter, a proportional and integral (PI) feedback controller, and an STM32F407VG digital controller. A detailed control system is presented where the gate signal generated from the maximum power point tracking system controls the duty cycle of switching pulses applied to the MOSFET of the DC-DC converter and also ensures maximum utilization of the solar photovoltaic source. The PI controller produces the switching pulses for the flyback inverter by adjusting the inverter switches' duty cycle according to the inverter's output signal. The flyback inverter produces pure sinusoidal output voltage and current signals by adjusting the duty cycle according to the control signals generated through the STM32F407VG digital controller. The STM controller assures the sinusoidal output of the inverter even at lower solar radiation. The proposed model is developed in MATLAB/Simulink. A 300W digitally controlled flyback inverter prototype has been implemented using an STM32F407VG digital controller using the waijung blockset to verify the feasibility of the proposed scheme.*

Keywords *- Flyback inverter, Maximum power point tracking (MPPT), Perturb and observe method(P&O), Photovoltaic (PV) system, Pulse width modulation (PWM).*

1. Introduction

Over the past several years, the availability of limited non-renewable energy sources, climate change, and global warming have become critical issues worldwide.[1] According to the evidence from 21 European countries, it was found that the utilization of non-renewable energy sources also harms economic growth. [2-4] Fossil fuels contributed 73.5% of worldwide electricity production in 2017. Conversely, renewable sources contributed only 26.5%. [5, 12] Renewable energy sources such as solar, wind, and biomass are abundantly available worldwide and can reduce global warming. [6, 7] Developing countries should shift to renewable energy resources to reduce air pollution and protect the environment. [8-11] The sun being a constant energy source in most countries in the world, solar energy can be used as a renewable energy source for most applications. [8] Efficient use of solar energy under changing weather conditions is one of the significant challenges worldwide. Accordingly, a solar photovoltaic (SPV)-based system is implemented in this research work.

Due to the advantages of the flyback inverter like simplicity, low cost, and high efficiency, it is gaining more popularity currently. A review of the flyback inverter follows. A single-phase grid-connected system using a DC/DC flyback converter with a proportional-integral (PI) controller, a single-phase full-bridge inverter with a sinusoidal pulse width modulation (SPWM) switching technique, and a phase lock-loop (PLL) is implemented in MATLAB to reduce the total harmonic distortion from 52.45 % to 1.82%. [13] The flyback microinverter is designed in MATLAB Simulink with an H5 inverter controlled sinusoidal pulse width modulation (SPWM) with a PI controller. 2.59% THD is obtained with 94.08% efficiency. [14] An MPPT-based grid-connected photovoltaic system using a flyback converter is implemented in [15]. The output voltage and current waveform are produced with THD at 1.60% and 1.26%, respectively. A new switched-capacitor nine-level inverter based on a flyback DC-DC converter is presented to reduce the number of switches, diodes, and required

independent DC sources. [16] The results are verified in PSCAD software.

Many researchers have worked on digital control techniques, and it has been observed that applying a digital controller to any inverter improves the system's performance. A literature review on digital control techniques is discussed below. A TMS320F2812 DSP controller controls the inverter's switching for performance improvement.[17] A control method is implemented to improve the efficiency of the flyback inverter, which controls the active clamp circuit and each converter phase of an inverter according to the output power of the PV module.[18] A new topology of a digital controller TMS320C28027 to a bidirectional high-frequency link photovoltaic inverter has been implemented for photovoltaic application using a perturb and observation(P&O) method. The THD observed in this method is 4.95%.[19] A PWM signal is generated using a DSP controller to control the voltage source inverter.[20] The THD is obtained below 5%. An FPGA-based SPWM controller is implemented for a single-phase solar inverter to reduce the complexity and cost of the system.[21] A novel approach is presented to model and simulate a closed-loop maximum peak power tracking (MPPT) based single phase stand-alone system using particle swarm optimization (PSO) technique to reduce the THD value.[22]

The review shows that the digital controller improves the system's performance under standard solar radiation. [18-22] The presented research work also utilizes the digital control technique for performance improvement at low radiation. In [13-16], the flyback inverter is implemented in MATLAB, but experimental validation was not carried out. This research presents an SPV-based system that utilizes the P&O method of maximum power point tracking to track maximum power from the solar panel. The SPV output is applied to the DC-DC converter. The proportional and integral (PI) controller is implemented by using the STM32F407VG digital controller card. The controller generates the PWM pulses, which control the switching of the insulated gate bipolar transistor (IGBT)s of the flyback inverter. The system produces pure sinusoidal output voltage and current waveforms. It has been observed that using the STM controller and waijung platform; the system maintains a proper sinusoidal output signal at lower radiation, which shows the novelty of the research work. The system is first implemented in MATLAB, and extensive experiments validate the results.

2. System Configuration and Working

Fig.1 presents the block diagram and system configuration of the solar-based digitally controlled flyback inverter.

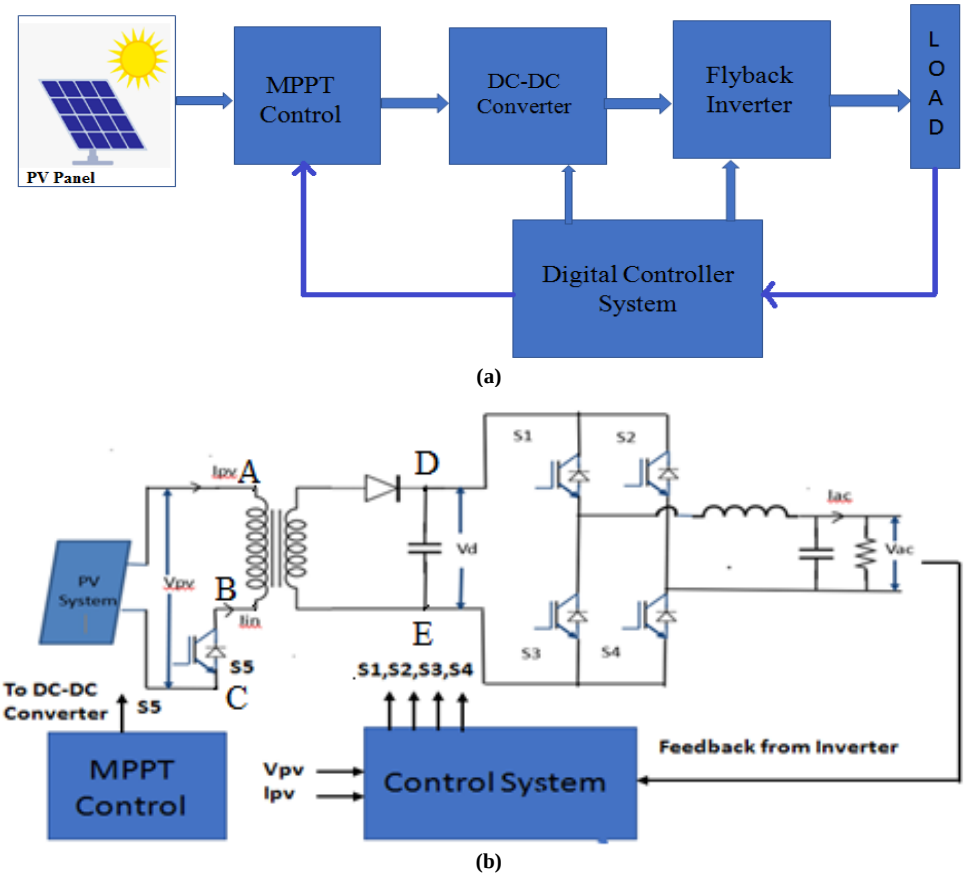

Fig. 1 Proposed system
(a) Block diagram, (b) System configuration of flyback inverter

An arrangement to connect the digital control system with the solar-based flyback inverter is created in the presented system to improve the ac output voltage and current of the flyback inverter. The solar PV system senses the PV current and voltage. The P&O method of the MPPT system tracks the maximum voltage and is fed to the DC-DC converter. The primary winding of the flyback transformer is connected with the PV system through an input capacitor. This input capacitor avoids zero current flowing in the flyback inverter. The secondary winding of the transformer is connected with the single-phase inverter. Switches S1, S2, S3, and S4 build the single-phase inverter. Point D on the system prototype is connected to the collector of switches S1 and S2, which are interconnected. Emitters of S3 and S4 switches are joined and connected at point E. The switching of these switches is controlled by utilizing the PWM signals generated by the digital controller card (Nitech make). The two legs of the single-phase inverter are interleaved utilizing an inductor and capacitor, which creates the LC filter. The LC filter removes the ripples present in the output of the flyback inverter and generates the pure sinusoidal output signal. The current transformer and power transformer are utilized for observing the output signals.

3. Design of the System

The system is designed for 300W power, input voltage 72 to 82V, IGBT rating 1200V, and switching frequency 10kHz. [28,29] The system components, viz SPV source, flyback transformer, and LC filter, are accordingly designed in the following steps.

3.1. Step 1: selection of the SPV source

The required power is 300W. Therefore, the 150Wp SPV module is selected with an open-circuit voltage (Voc) 44.30V, short circuit current (Isc) 4.51A, the voltage at maximum power (Vmp) 36.10V, current at maximum power (Imp) 4.16A, module efficiency (n) 12.89%.
Number of modules connected in series = 2

3.2. Step 2: Design of DC-DC converter

The DC-DC converter design consists of a flyback transformer design, diode selection and capacitor, which is discussed in the following sections.

3.2.1 Flyback Transformer Design:

$$Prim\ voltage = IGBT\ Ratings - Max.input\ voltage \quad (1)$$

$$V_{reflected} = 0.7 \times 1200 - \sqrt{2} \times 82 = 724V$$

Minimum peak voltage

$$V_{in_{min_{pk}}} = \sqrt{2} \times V_{in_{min}} = \sqrt{2} \times 72 = 101.8V \quad (2)$$

Maximum duty cycle

$$D_{max} = \frac{V_{reflected}}{V_{reflected} + min.peak.voltage} \quad (3)$$

$$D_{max} = \frac{724}{724 + 101.8} = 0.8767$$

Minimum input current

$$I_{in_{max}} = \frac{300}{0.8 \times 72 \times 0.9} = 5.787A \quad (4)$$

Peak input current

$$I_{in_{max_{peak}}} = \sqrt{2} \times I_{in_{max}} = \sqrt{2} \times 5.787 = 8.184A \quad (5)$$

Peak primary current

$$I_{p_{peak}} = \frac{2 \times 8.184}{0.8767} = 18.67A \quad (6)$$

Primary Inductance

$$L_p = \frac{0.8767 \times 101.8}{18.67 \times 20 \times 10^3} = 239.01uH \quad (7)$$

Transformer turn ratio

$$\frac{N_p}{N_s} = \frac{V_1}{V_2} = 4 \quad (8)$$

3.3. Step 2: Design of LC filter

The LC filter converts the chopped inverter output into the sinusoidal ac output in the presented system.
The inductor and capacitor values of the LC filter are estimated as

The switching frequency of the inverter is

$$f_{sw} = 10kHz$$

The cut-off frequency of the LC filter is

$$fc = 2kHz$$

$$F_c = \frac{1}{2 \times \pi \times \sqrt{LC}} \quad (9)$$

$$C = \frac{1}{4 \times \pi^2 \times L \times {F_c}^2} \quad (10)$$

If the inductor is selected as: $L = 2.5mH$

$$C = \frac{1}{4 \times \pi^2 \times 2.5 \times 10^3 \times 2000^2} = 2.5uF \quad (11)$$

4. Control system

The presented system consists of two controlling actions. The first control scheme is the P&O MPPT algorithm which controls the switching of the IGBT of the DC-DC converter. The second controlling action represents the switching of the flyback inverter. The two control actions are discussed in detail in the following section.

4.1. MPPT Scheme

In general, four MPPT methods are available. Fractional open circuit voltage, fractional short circuit current, incremental conductance, and P&O method. In the presented system, the P&O method of the MPPT algorithm is implemented to obtain the maximum output from the PV system due to its simplicity and accuracy. [23-24, 30]

The MPPT system observes the output voltage(V_{pv}) and current(I_{pv}) from the solar panel and the PV power (P_{pv}) is calculated using the values of (V_{pv}) and (I_{pv}). PV voltage and power are periodically measured and

compared with the previous values of voltage$(V_{pvold})$and power(P_{pvold}). The difference between the current and previous values of voltage and power are calculated and are given by ΔV and ΔP, respectively. The P&O algorithm examines the ratio $\Delta P/\Delta V$ and decides the change in power. Four cases are represented in Table 1 by considering the sign of ΔV and ΔPsuch that maximum power is generated from the PV system.

Table 1. Possible variation in DC voltage to increase PV power

Case	ΔP	ΔV	ΔP/ΔV	Change in Vdc	Response
I	+ ve	+ ve	+ ve	$V_n(k)\uparrow$	$P_{pv}\uparrow, V_n(k)\uparrow$
II	- ve	- ve	+ ve	$V_n(k)\uparrow$	$P_{pv}\uparrow, V_n(k)\uparrow$
III	+ ve	- ve	- ve	$V_n(k)\downarrow$	$P_{pv}\uparrow, V_n(k)\downarrow$
IV	- ve	+ ve	- ve	$V_n(k)\downarrow$	$P_{pv}\uparrow, V_n(k)\downarrow$

In case I and case II, $\Delta P/\Delta V$is positive and the PV power is increased by raising the PV voltage V_{pv}. In case III and case IV, $\Delta P/\Delta V$ is negative, and the PV power is increased by decreasing the PV voltage V_{pv}.Thus, maximum power tracking has been carried out by monitoring the $\Delta P/\Delta V$ and accordingly changing the V_{pv}value. To achieve this, the P&O scheme is realized by the following equation:

$$V_n(k) = V_n(k-1) + \Delta V, \quad \frac{if\,\Delta P}{\Delta V} > 0 \tag{12}$$

$$V_n(k) = V_n(k-1) - \Delta V, \qquad if\ \Delta P/\Delta V < 0 \tag{13}$$

where $V_n(k-1)$ and $V_n(k)$represents the previous and current values of the PV voltage, respectively, and ΔV represents the incremental value of the PV voltage. The value $V_n(k)$ derived from (12) and (13) is used as the reference voltage to control the DC-DC converter. The DC-DC converter dynamically adjusts the DC voltage and maximizes the power generated by the PV source.

4.2. Control of flyback inverter

From the literature survey, it has been observed that the performance of the inverter can be improved by applying the digital control technique. Therefore, in this study, the PI controller controls the duty cycle of switching pulses to trigger the flyback inverter switches to improve their performance.

The PI controller is formed by combining proportional and integral control actions. In this case, the control signal shows proportionality with the error signal and the integral of the error signal. The mathematical representation of the proportional plus the integral controller is given below as in [25-27, 31].

$$\boldsymbol{m(t) = K_p.e(t) + K_i \int e(t)} \tag{14}$$

Where $\boldsymbol{K_p}$ is proportional constant
K_i is an integral constant
$e(t)$ is an error signal.

The details of the implemented PI controller are given below.

The voltage derived in (12) and (13) is compared with the DC bus voltage V_{dc} and an error signal is produced. This error signal is reduced by utilizing the PI controller. The PI controller is designed with a proportional gain of 1 and an integral gain of 20, which produces the signal with a modulation index M_a and this varies from 10 to 99. A three-phase sine generator generates a continuous positive sequence by considering the error signal with the fundamental frequency of 50Hz. The output of the PI controller is the reference signal, and it is expressed as

$$V_{err}[n] = (V_{pv}[n] - V_{dc}[n]) \tag{15}$$

$$D[n] = D[n-1] + K_p(V_{err}[n] - V_{err}[n-1]) + K_i.Ts.V_{err}[n] \tag{16}$$

where D represents the duty cycle. This signal is compared with the high-frequency carrier signal to generate SPWM pulses. These pulses control the switching of the flyback inverter.

5. Waijung Platform

The Waijung blockset is a Simulink blockset that can be used to easily and automatically generate C code from MATLAB/Simulink simulation models for many kinds of microcontrollers.

In this research work, the waijung blockset has been specifically designed to support the STM32F4 family of microcontrollers, a high-performance and digital signal processor microcontroller unit from STmicroelectronics. [32] This blockset generates the C code for the digital controller STM32F407VG from the Simulink model of the PI controller designed in MATLAB.

6. Results and Discussion

6.1. Software Results

Fig. 2 shows the simulation model of the presented system.

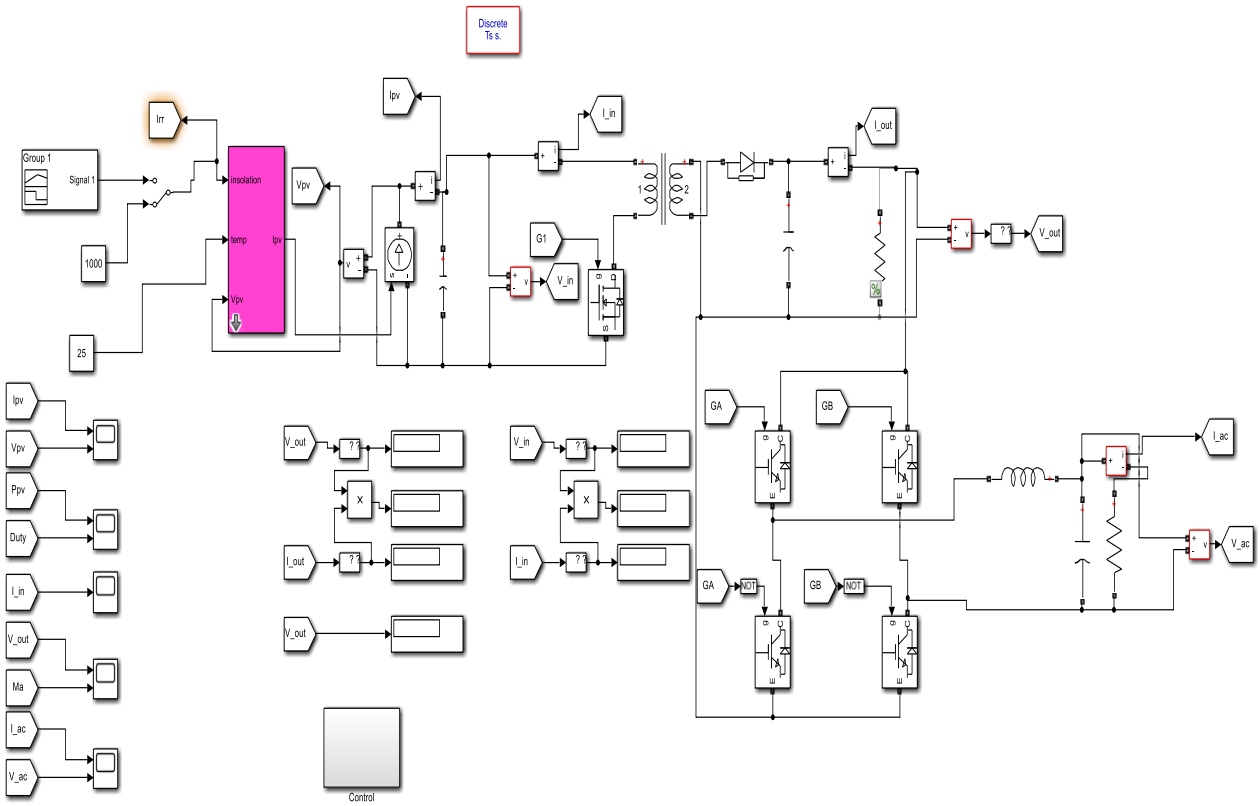

Fig. 2 Simulink Model of MPPT-based digitally controlled closed-loop flyback inverter

The model consists of a PV system, a DC-DC converter, a flyback inverter, an LC filter, and the control system. The PV system is developed by connecting 72 series cells and 1 parallel cell. The system shows an open-circuit voltage of 44.30 V (Voc) and a short circuit current of 4.51 A (Isc). Fig. 3(a) and 3(b) show the PV output current, the PV output voltage, the PV output power, and the duty cycle, respectively. The PV system uses insulation of 1000W/m2. The DC-DC converter comprises a flyback transformer, an IGBT switch, a diode, and a dc-link capacitor. The flyback transformer is designed with a turn ratio of 4:1, a nominal power of 10kW, and a frequency of 20 kHz. The converter produces the dc output voltage as shown in fig.4. Four IGBT switches with an anti-parallel diode, minimum internal resistance, and 100kohm snubber resistance are connected to form a single-phase inverter topology. This single-phase inverter converts the input dc signal into a pure ac sinusoidal signal. The LC filter is designed with an inductance of 2.5mH and a capacitance of 2.5uF. The control block produces two control signals. One with a switching frequency of 20kHz, which controls the duty cycle of IGBT of the DC-DC converter and the second with a switching frequency of 10kHz, which controls the duty cycle of the IGBT switches of the single-phase flyback inverter. Fig.3 illustrates the performance of the PV model by showing the PV current, the PV voltage, the PV power and the duty cycle of the switching pulses. Fig.5 shows the ac output current and voltage of the flyback inverter.

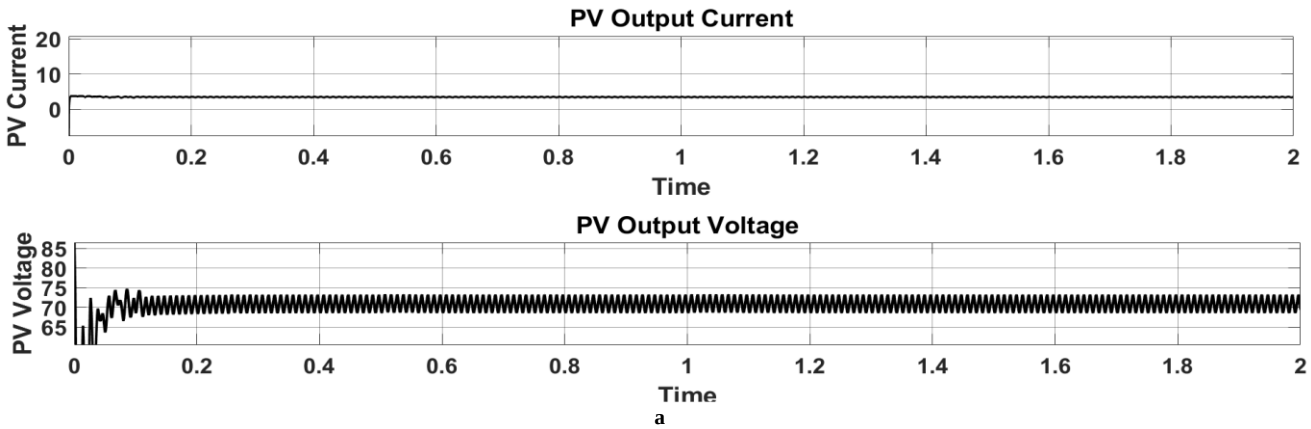

a

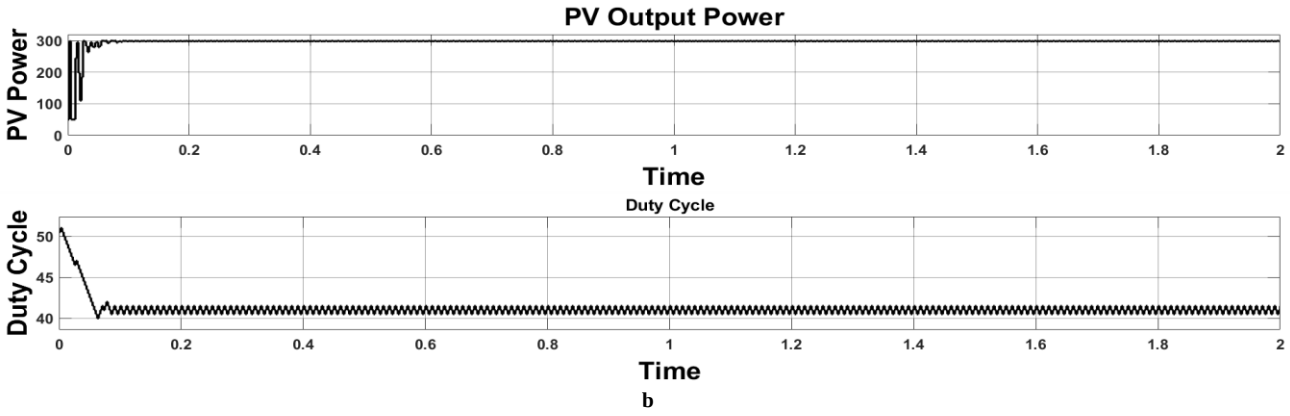

Fig. 3 Performance of the PV model
(a)At 1000W/m^2 solar radiation: Ipv, Vpv, (b) At 1000W/m2 solar radiation Ppv, D

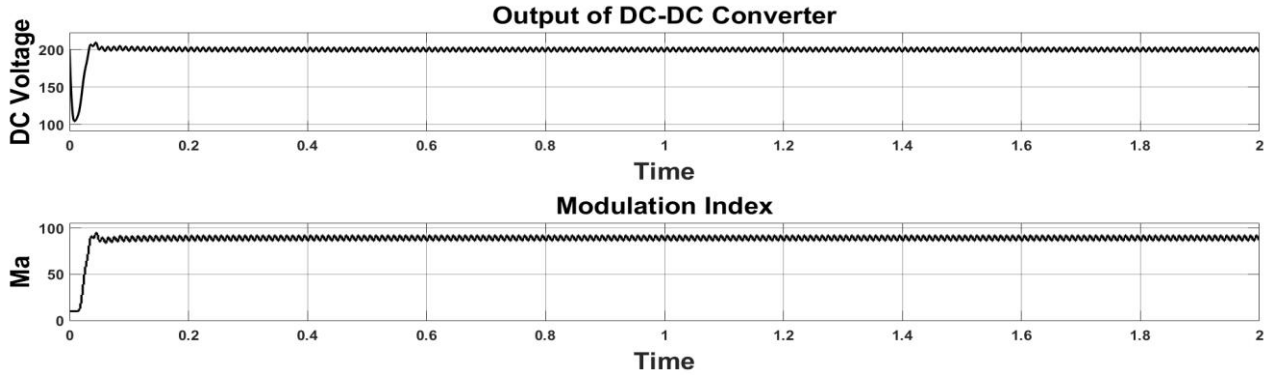

Fig. 4 Performance of the dc-dc converter model Vdc, Ma

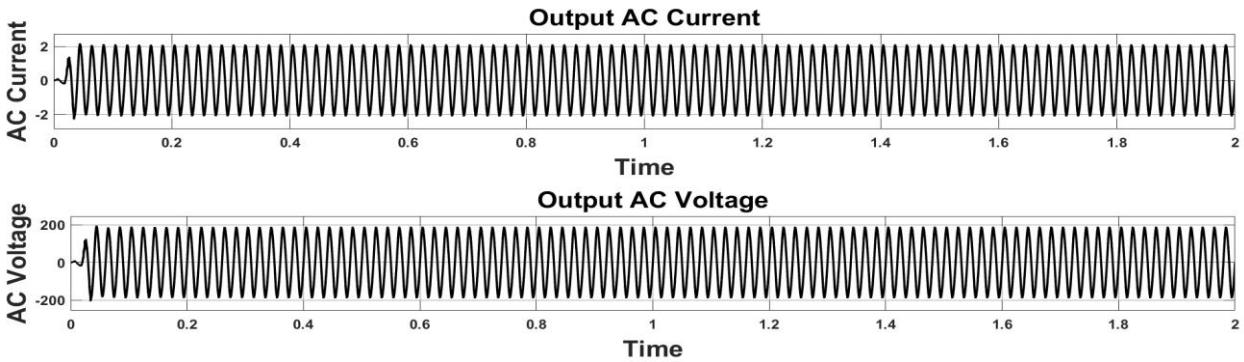

Fig. 5 Performance of the flyback inverter Iac, Vac

6.2. Experimental results

Fig.6 shows a line diagram and photograph of the experimental setup. The PV system is connected at one end of the dc-dc converter (Nitech make) through three devices, a transfer switch, an input capacitor of 1000uF, and an input resistor of 1ohm 20W. The input capacitor prevents the zero current from flowing in the flyback inverter. The input resistor is used for measurement purposes. A Hall effect sensor card (Nitech make) is utilized to sense the PV voltage, current, and DC-bus voltage. The solar PV source is connected with the converter's primary side of the flyback transformer (Nitech make). A DC link capacitor of 100uF, 450V is connected at the output side of the DC-DC converter. The DC-DC converter is connected with a single-phase inverter. In the setup, the single-phase inverter consists of a two-level IGBT-based inverter, an intelligent Infineon IC-based IGBT driver card, and a DC-bus current and voltage sensor card (Nitech make). The test results are observed by using a four-channel digital storage oscilloscope.

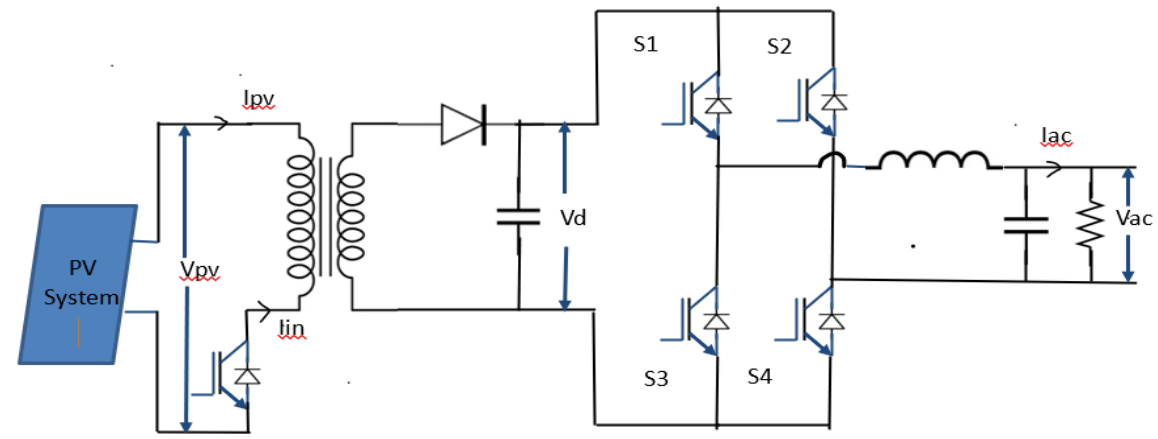

(a)

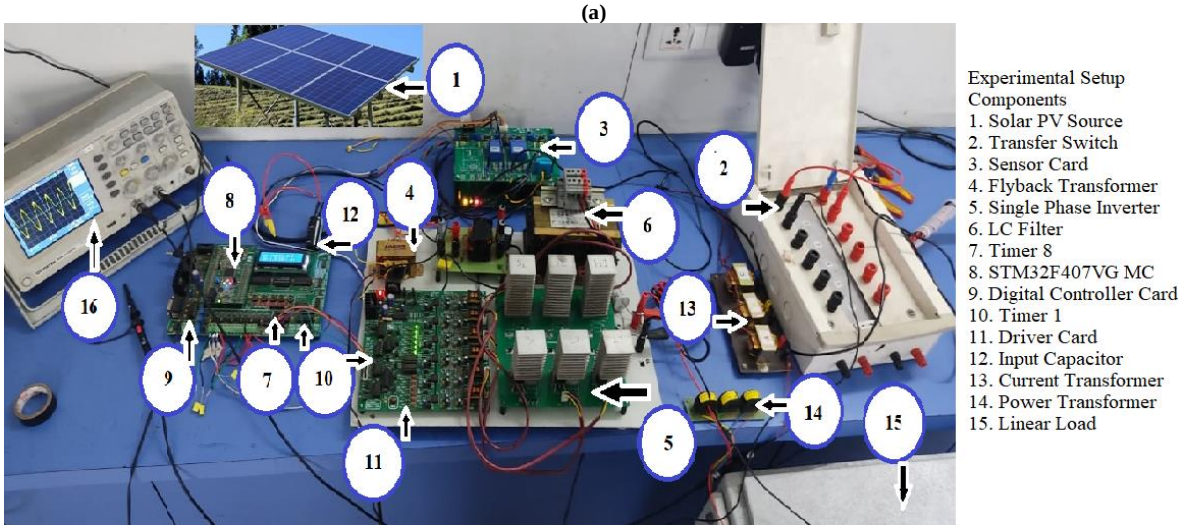

(b)

Fig. 6 Experimental prototype of the digitally controlled flyback inverter (a)Line diagram, (b) Photograph

In the experimental setup, the PV voltage (Vpv), the PV current (Ipv), the DC-bus voltage (Vdc), the duty cycle (D), modulation index (Ma), the load voltage (Vac), and the load current (Iac) are sensed to monitor the performance of the system. The Ipv, the Vpv, and the Vdc, sensed by utilizing the sensor card, are fed to the 1, 2, and 3 pins of an analogue-to-digital converter of the generic ARM Cortex-M4 32-bit microcontroller (STM32F407VG). This board deploys the digital controller card (Nitech make). The on-chip advanced PWM timers (Tim-1 and Tim-8) generate the two control signals. Tim-1 generates high-frequency PWM pulses at 10 kHz for the single-phase inverter; however, Tim-8 generates the PWM signal at 20 kHz for the DC-DC converter switch. The intermediate control signals can be observed using the on-chip digital-to-analogue converter pins. Pins PC6, PA7, PC7, and PB0 of the inverter timer are connected to the H1, L1, H2, and L2 pins of the inverter, whereas pin PA8 of the flyback timer is connected to the H3 pin of the switch of the DC-DC converter. These pins provide the switching pulses to the IGBTs. The Infineon IC-based silicon carbide (SiC) driver card is utilized to drive the SiC IGBT switches. The voltage of high-frequency PWM pulses varies between 0V to 5V. Accordingly, this driver card converts the pulse voltage to vary between -8V to +15V to drive the SiC IGBT switches. The flyback inverter generates a chopped AC output signal. Hence, the LC filter converts the chopped AC signal into a pure sinusoidal AC signal. The detailed ratings of the components used in the experimental setup are given in Table 2.

Table 2. Experimental setup components and control parameters

Parameter	Value
DC-bus	
DC-bus voltage	200 V
DC link capacitance C_2	100 uF
SPV Source	
SPV Model	Waaree 150
Peak power	150 Wp
The voltage at maximum power (Vmp)	36.10 V
Current at maximum power (Imp)	4.16 A
Number of modules connected in series	2
Peak power of designed SPV	300 Wp
DC-DC converter	
Duty cycle	0.8767
Switching frequency	20 kHz
Flyback transformer	
Peak current	18.67 A
Inductor (Lp)	239.01 uH

Turn ratio	4:1
Duty cycle	0.8767
IGBT Inverter Module	
IGBT	25N120
Voltage rating	1200 V
Switching frequency	10 kHz
LC filter	
Inductor (L)	2.5 mH
Capacitor (C)	2.5 uF

Extensive experiments investigate the implemented system's performance on the setup. The results are captured under different test conditions. The tests are accompanied in three parts to verify the system's feasibility. 1) Steady-state performance (for lower solar radiation 2) Steady-state performance (for higher solar radiation), and 3) Dynamic performance

6.2.1. Test-1: Steady-state performance of the system (For lower solar radiation: 247W/m2)

Fig. 7 illustrates the steady-state performance of the flyback inverter at 247W/m2 solar radiation. In Fig. 7a, the PV voltage is 60V, and the PV current is 0.6A. Thus, 36W power is generated at 247W/m2 with a 0.40 duty ratio, as shown in fig. 7b. The input current is shown in Fig. 7c. At the given solar radiation of 247W/m2, the corresponding DC bus voltage of 200V is generated, which is MPP voltage. The modulation index is 32, as illustrated in Fig. 7d. The load current is 0.7A, and the load voltage is 38V, as presented in Fig. 7e, which is the inverter ac output signal at 247W/m2.

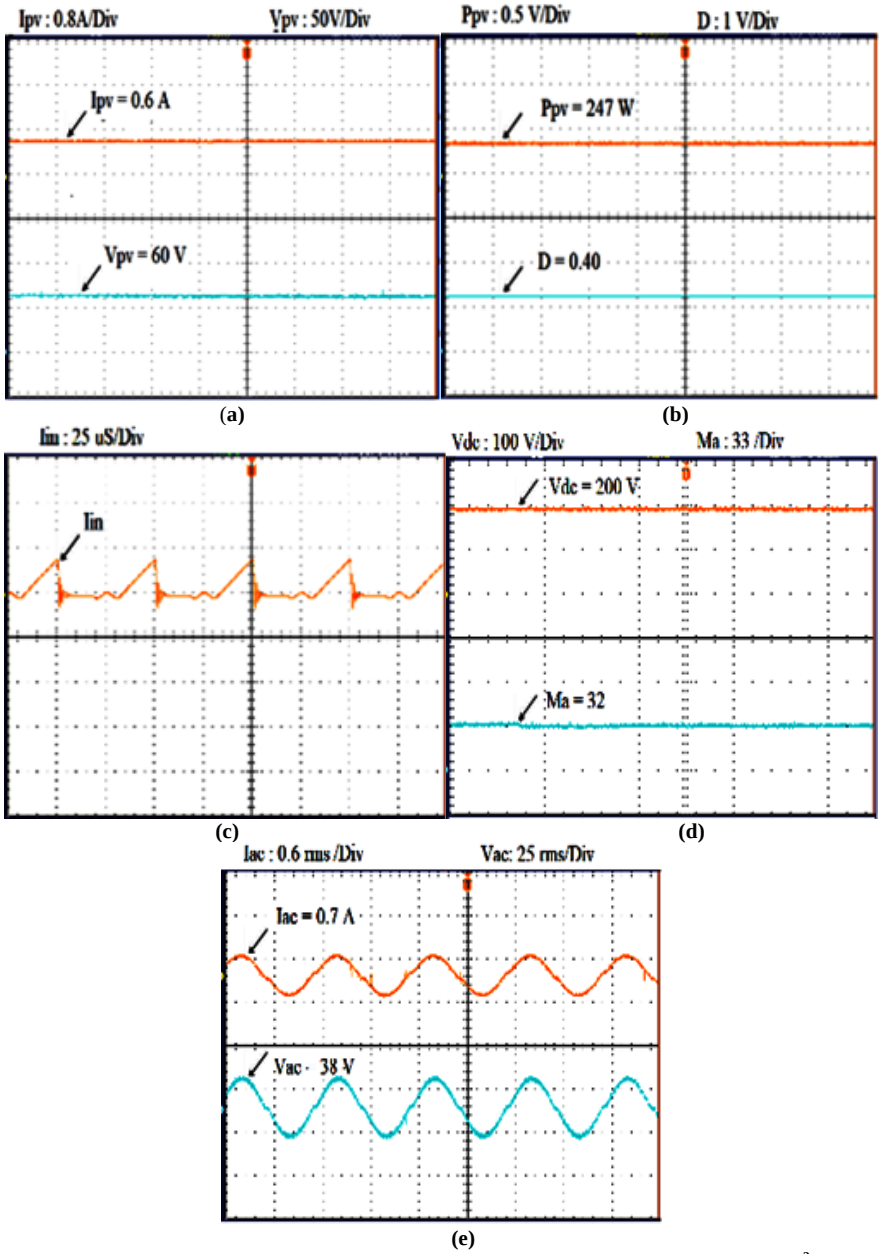

Fig. 7 steady-state performance of the system (for lower solar radiation: 247W/m^2)
(a)PV current, PV voltage, (b) PV power, Duty cycle, (c)Input current, (d)DC voltage, Modulation index, (e)AC current, AC voltage

6.2.2. Test-2: Steady-state performance of the system (For higher solar radiation: 825W/m2)

Fig. 8 demonstrates the steady-state performance of the flyback inverter at 825W/m2 solar radiations. In Fig. 8a, the PV voltage is 75V, and the PV current is 3.3A. The PV system generates a power of 247.5W with a duty ratio of 0.50 as presented in Fig. 8b. The input current is given in Fig. 8c. A DC bus voltage of 200V is generated, which is MPP voltage at the given solar radiation at 825W/m2 and the modulation index is 87 as illustrated in Fig. 8d. The load current is 1.91A. The load voltage is 110V, as presented in Fig. 8e, which is the ac output signal of the flyback inverter at 825W/m2. Table 3 provides a comparison between the simulation and experimental results.

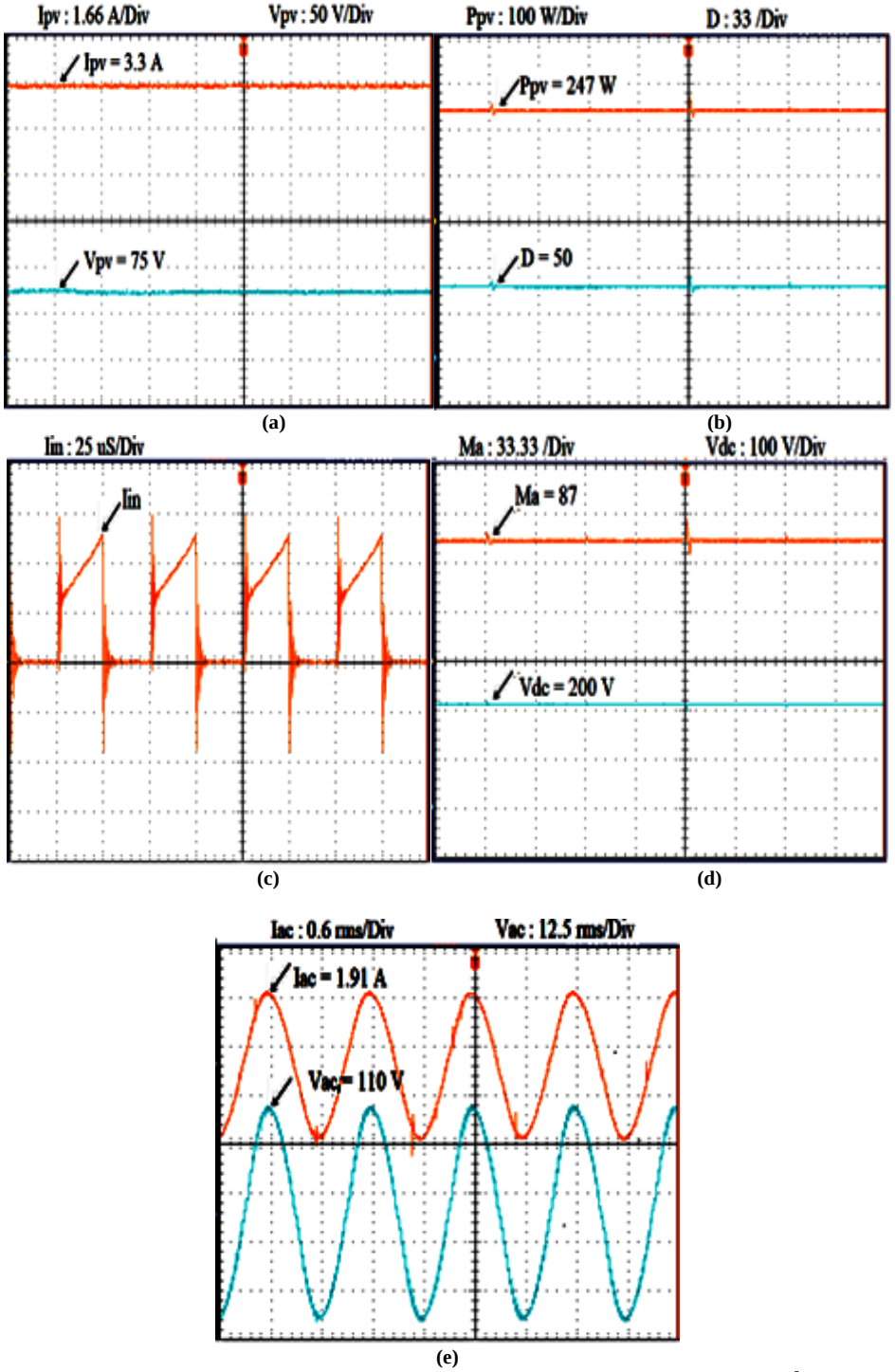

Fig. 8 steady-state performance of the system (for higher solar radiation: 825W/m^2)
(a)PV current, PV voltage, (b) PV power, Duty cycle, (c)Input current, (d) Modulation index, DC voltage, (e)AC current, AC voltage

Table 3. Comparison of simulation and experimental results for 825W/m^2 solar radiation

Parameters	Simulation Results	Experimental Results
Ipv	3.45mA	3.3 mA
Vpv	70.94 V	75 V
Ppv	245.1	247.5
D	42	50
Iin	0.64 A	--
Vdc	200 V	200 V
Ma	83	87
Iac	1.88	1.91 A
Vac	150 V	110 V

6.2.3. Test-3: Dynamic performance of the system (For variable sun radiation)

Fig. 9 illustrates the dynamic performance of the flyback inverter at variable solar radiation. In Figs. 9a and 9b, the PV current, voltage, power, and duty cycle continuously vary concerning the variable solar radiation. The modulation index changes with variable solar radiation and the DC bus voltage is constant at 200V at variable solar radiation, which is also the MPP voltage presented in Fig. 9c. Fig. 9d shows the variation in the load current and the load voltage, which is the ac output signal of the flyback inverter at variable solar radiation. Fig. 9e and 9f show the expanded portion of the load current and the load voltage at positions 49.00% and 66.76%, respectively.

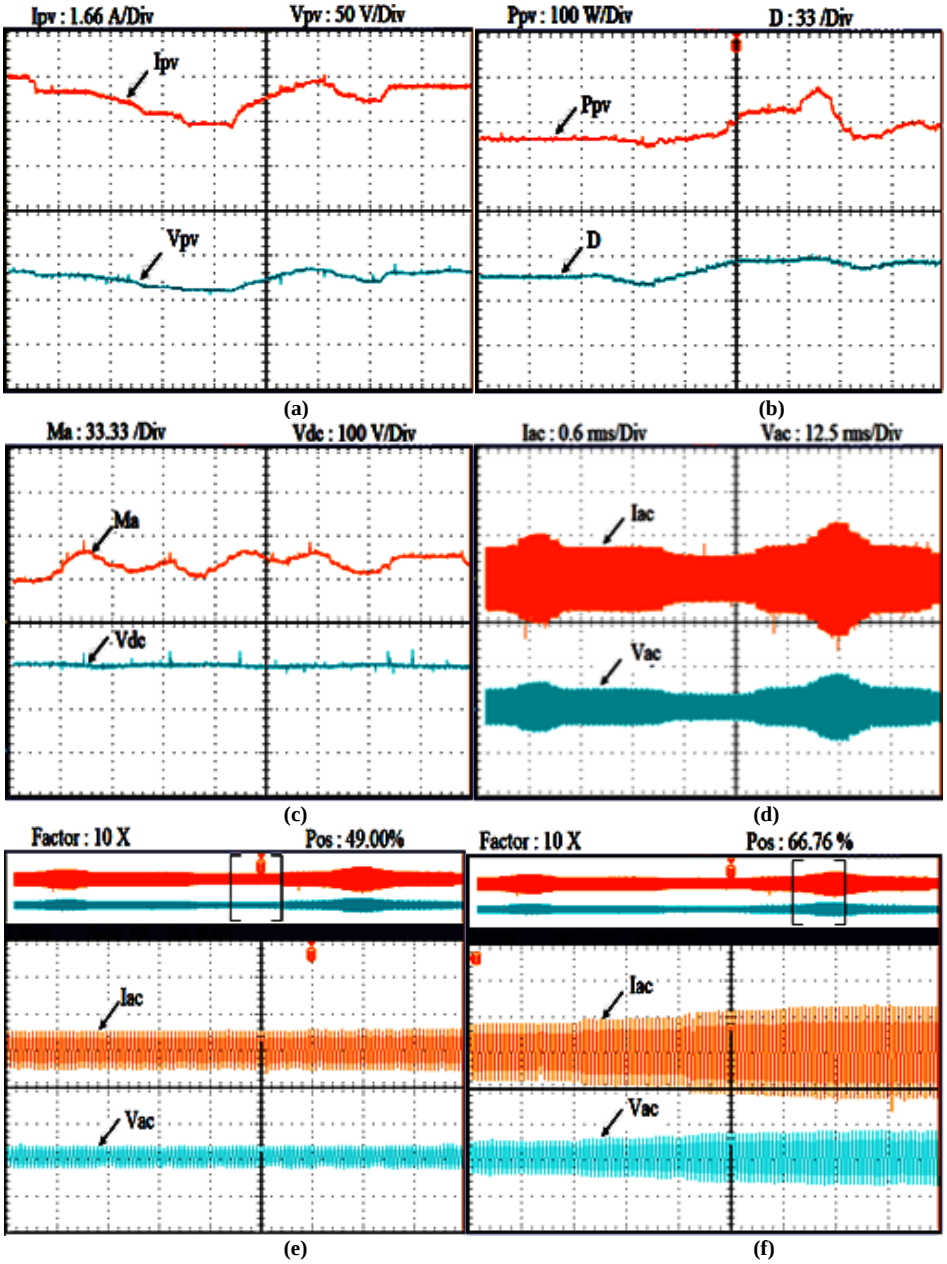

Fig. 9 Dynamic performance of the system
(a)PV current, PV voltage, (b) PV power, Duty cycle, (c)Modulation index, DC voltage, (d)AC current, AC voltage, (e)49% expanded portion and (f)66.76% expanded portion of AC current, AC voltage

On observing 1) Steady-state performance (for lower solar radiation, 2) Steady-state performance (for higher solar radiation), and 3) Dynamic performance, it has been observed that utilization of the controlling system, i.e. STM32F407VG digital controller, maintains the performance of the flyback inverter for lower radiation of 247W/m^2.

7. Conclusion

A novel method is implemented for MPPT-based photovoltaic closed loop flyback inverter. The solar photovoltaic system with the P&O method of MPPT is designed to operate at peak power and extract the maximum power from the SPV system. A digital control system is implemented to control the switching of IGBT switches of the flyback inverter. A single-phase topology of the flyback inverter is utilized in this research work. The complete system is designed and implemented in MATLAB/Simulink. The system's feasibility is tested by creating the prototype in the laboratory. A novel method is utilized for implementing the MPPT-based photovoltaic closed loop flyback inverter with an STM32F407VG controller using the waijung tool. A Digital controller card (Nitech make) with STM32F407VG generates the two control signals for controlling the switching of the IGBT switches of the DC-DC converter and the flyback inverter. The control signal adjusts the duty cycle according to the output of the flyback inverter to minimize the error signal and produce an improved output. The presented system produces the improved pure sinusoidal ac output voltage and current for linear and non-linear load at lower solar radiation of 247W/m^2. The experimental results of inverter operation validate the feasibility of the system. The simulation results and experimental results match exactly. In today's era of renewable energy, the proposed model with the PV system's implementation will benefit society, thus promoting the use of renewable energy resources and reducing the system's complexity and cost.

Acknowledgement

The authors would like to thank National Infotech, Surat, (Gujrat), India, for providing the technical support for the research project under the "Memorandum of Understanding" between National Infotech, Surat, (Gujrat) and SSBT's College of Engineering and Technology, Bambhori, Jalgaon, (M.S.), India.

References

[1] AnamAzam, Muhammad Rafiq, et al., "Analyzing the Effect of Natural Gas, Nuclear Energy and Renewable Energy on GDP and Carbon Emissions: A multi-variate Panel Data Analysis", 2020. Doi-10.1016/j.energy.2020.119592.

[2] Benjamin AmpomahAsiedu, AbisolaAmudat Hassan and Murad A. Bein, "Renewable Energy, Non-Renewable Energy, and Economic Growth: Evidence from 26 European Countries," *Environmental Science and Pollution Research,* 2020. Doi-10.1007/s11356-020-11186-0.

[3] Anwar Khan, et al.: "Impact of Technological Innovation, Financial Development and Foreign Direct Investment on Renewable Energy, Non-Renewable Energy and the Environment in Belt & Road Initiative Countries," *Renewable Energy*, vol. 171, pp. 479-491, 2021.

[4] Aparna Sawhney, "Striving towards a Circular Economy: Climate Policy and Renewable Energy in India", *Clean Technologies and Environmental Policy,* vol. 23, pp. 491-499, 2020.

[5] AtikaQazi, et al.: "Towards Sustainable Energy: A Systematic Review of Renewable Energy Sources, Technologies, and Public Opinions," *IEEE Access,* vol.7, pp. 63837-63851, 2019.

[6] ElzbietaKacperska, et al., "Use of Renewable Energy Sources in the European Union and the Visegrad Group Countries—Results of Cluster Analysis," *Energies,* 2021. *Crossref,* https//doi.org/10.3390/en14185680

[7] Rajvikram Madurai Elavarasan, et al., "A Holistic Review of the Present and Future Drivers of the Renewable Energy Mix in Maharashtra, State of India", Sustainability, vol. 12, pp. 6596, 2020. *Crossref,* htttps://doi.org//10.3390/su12166596.

[8] Muhammad Mohsin, et al., "Assessing the Impact of Transition from Non-Renewable to Renewable Energy Consumption on Economic Growth-Environmental Nexus from Developing Asian Economies," *Journal of Environmental Management*, 2021. *Crossref,* https//doi.org/10.1016/j.jenvman.2021. 111999.

[9] Fabien Chidan and Robert, et al., "A Critical Review on the Utilization of Storage and Demand Response for the Implementation of Renewable Energy Microgrids," Sustainable Cities and Societies, vol. 40, pp. 735-745, 2018.

[10] George E. HalkosandEleni-Christina Gkampour, "Reviewing Usage, Potentials, and Limitations of Renewable Energy Sources," *Energies,* vol. 13, pp. 2906, 2020. Doi:10.3390/en13112906.

[11] Dayong Zhang, et al., "Board Characteristics, External Governance and the Use of Renewable Energy: International Evidence," *Journal of International Financial Markets, Institutions & Money,* 2021. Doi:10.1016/j.intfin.2021.101317.

[12] International Energy Agency, "World Energy Outlook –Analysis," 2021.

[13] A.A. Bakar, et al., "Modeling of Single-Phase Grid-Connected using MATLAB/Simulink Software," *IEEE Student Conference on Research and Development,* pp. 69-74, 2019. Doi:10.1109/SCORED.2019.8896226

[14] ErsanKabalci, et al., "Design and Analysis of a Flyback Micro Inverter with H5 Inverter," *1st Global Power, Energy and Communication Conference,* pp. 368-373, 2019. Doi: 10.1109/GPECOM.2019.8778530.

[15] MD. ModassirMasoom, et al., "MPPT Based Grid Connected Photovoltaic System Using Flyback Converter," *IEEE International Conference for Innovation in Technology (INOCON),* Bengaluru, India, 2020. Doi: 10.1109/INOCON50539.2020.9298412.

[16] MiladGhavipanjehMarangalu, et al., "A new Switched Capacitor Nine-Level Inverter Based on Flyback DC-DC converter," *22nd IEEE International conference on Industrial Technology,* pp. 266-271, 2021. Doi: 10.1109/ICIT46573.2021.9453520.

[17] H. S. Bae, et al., "Current Control Design for a Grid Connected Photovoltaic/Fuel Cell DC-AC Inverter," Twenty-Fourth Annual IEEE Applied Power Electronics Conference and Exposition, pp. 1945-1950, 2009. Doi: 10.1109/APEC.2009.4802939.

[18] Young-Ho Kim, et al., "A New Control Strategy for Improving Weighted Efficiency in Photovoltaic AC Module-Type Interleaved Flyback Inverters," *IEEE Transactions on Power Electronics*, vol. 28, no. 6, pp. 2688-2699, 2013. Doi: 10.1109/TPEL.2012.2226753.

[19] Prashant V. Thakre and Dr. SarojRangnekar, "Implementation of Digital Controller TMS320C28027 to MPPT Based Single Phase Bidirectional High Frequency Link Inverter for Photovoltaic Application," *International Journal of Renewable Energy Research*, vol. 4, no. 1, pp. 102-108, 2014.
[20] V. M. Deshmukh, A. J. Patil, and P. V. Thakre, "Development of Matlab/Simulink Model for Three Phase PWM Inverter and Hardware Implementation and Testing Using DSP with Non-linear Load," *International Journal of Control Science and Engineering*, 2015. Doi:10.5923/j.control.20150501.01.
[21] Ramanantsihoarana H. Nathalie, RastefanoElisée, "Implemented of FPGA based SPWM Controller for Single Phase Solar Inverter," *International Journal of Advance Research and Innovative Ideas in Education (IJARIIE)*, vol. 2, no. 6, pp. 1788-1795, 2016.
[22] P. V. Thakre and V. M. Deshmukh, "Modeling, Simulation and Experimental Investigation of Closed-Loop MPPT Based Single Phase Stand-Alone Photo Voltaic System Using Particle Swarm Optimization Technique," *International Journal of Engineering and Technology*, vol. 7, no. 2.21, pp. 94-98, 2018.
[23] Jacob James Nedumgatt et al., "Perturb and Observe MPPT Algorithm for Solar PV Systems-Modeling and Simulation", *Annual IEEE India conference*, 2011. Doi: 10.1109/INDCON.2011.6139513.
[24] ParimitaMohanty, et al., "MATLAB Based Modeling to Study the Performance of Different MPPT Techniques used for Solar PV System Under Various Operating Conditions*", Renewable and Sustainable Energy Reviews,* vol. 38, pp. 581–593, 2021.
[25] J. Surya Kumari, et al., "Design and Analysis of P&O and IP&O MPPT Techniques for Photovoltaic System," *International Journal of Modern Engineering Research (IJMER)*, vol. 2, no. 4, pp. 2174-2180, 2012.
[26] T.Ajithkumar, B.Karuppasamy, R.Aswinkumar, U.K.Balakannan, P.Nirmalkumar, "Implementing a Single Switch DC-DC Converter for Photo Voltaic System," *SSRG International Journal of Electrical and Electronics Engineering*, vol. 7, no. 4, pp. 19-22, 2020. Crossref, https://doi.org/10.14445/23488379/IJEEE-V7I4P105
[27] TufanDogruer, Nusret Tan, "Design of PI Controller using Optimization Method in Fractional Order Control Systems," *International Federation of Automatic Control (IFAC)*, vol. 51, no. 4, pp. 841-846, 2018.
[28] Durga Prasad Ananthu and DrNeelshetty K, "Generation and Economics of 100kwp Roof-Top Grid Connected PV Plan", *International Journal of Engineering Trends and Technology (IJETT)*, vol. 60, no. 3, pp. 158-162, 2018.
[29] BiksAlebachewTaye, "Design, Modeling and Control of Stand-alone Photovoltaic System for Rural Electrification in Ethiopia using MATLAB", *International Journal of Engineering Trends and Technology (IJETT)*, vol. 66, no. 3, pp. 184-190, 2018.
[30] Kavita Joshi et al., "Maximum Power Operation of a PV System Employing Zeta Converter with Modified P&O Algorithm", *International Journal of Engineering Trends and Technology (IJETT)*, vol. 70, no. 7, pp. 348-354, 2022.
[31] Srishti Sharma, RiteshDiwan, "ZETA Converter with PI controller", *International Journal of Engineering Trends and Technology (IJETT)*, vol. 67, no. 2, pp. 33-36, 2019.
[32] NimitaGajjar, TejasZaveri, and NaimishZaveri, "Low-Cost Implementation of PV-STATCOM for Non-Linear Load Using STM32F407VG Controller", *International Journal of Engineering Trends and Technology (IJETT)*, vol. 69, no. 9, pp. 212-219, 2021.
[33] K SmritiRao, Ravi Mishra, "Comparative Study of P, PI and PID Controller for Speed Control of VSI-Fed Induction Motor," *International Journal of Engineering Development and Research (IJEDR)*, vol. 2, no. 2, pp. 2740-2744, 2014.